Research Article

Autonomous Positioning Of Unmanned Aerial Vehicle (UAV) For Power Lines Insulator Detection

Sze Sin VOON[1], *Lee Chin KHO*[1,*], *Sze Song NGU*[1], *Annie JOSEPH*[1], *Kuryati KIPLI*[1]

[1]Department of Electrical and Electronic Engineering, Faculty of Engineering, Universiti Malaysia Sarawak, 94300 Kota Samarahan, Sarawak, Malaysia

voonszesinu@gmail.com, lckho@unimas.my, ssngu@unimas.my, jannie@unimas.my, kkuryati@unimas.my

*Corresponding author: Lee Chin KHO; lckho@unimas.my

DOI: 10.15598/aeee.v22i3.5526

Article history: Received Oct 30, 2023; Revised Apr 02, 2024; Accepted May 27, 2024; Published Sep 30, 2024.

Abstract. *The rapid expansion of power transmission infrastructure necessitates the development of efficient and accurate inspection methods. This paper proposes an autonomous positioning model for Unmanned Aerial Vehicles (UAVs) that can detect power line insulators on transmission lines to address this need. The proposed model leverages machine learning algorithms for autonomous detection of insulators. To determine the optimal stopping point and safety distance between the UAV and the insulator, a mathematical model is presented that utilises the captured images and the machine learning algorithm. A simulation model is utilised to verify the proposed model, ensuring that the UAV moves to the best-predicted position. The machine learning algorithms are utilised to identify and calculate the length of power line insulators. A set of labelled insulator images is trained in the selected machine learning algorithm, enabling it to accurately determine the length of insulators in new images. The mathematical model considers the size of the insulator in the image to calculate the safety distance between the UAV and the power line insulator, while also determining the optimal image shooting coordinate. MATLAB's Simulink software is utilised to leverage the UAV's navigation and control systems, enabling it to move to the best position for capturing high-quality photos of the power transmission lines. The model also considers environmental conditions and operational constraints for optimisation. The proposed autonomous positioning model has undergone extensive simulation to demonstrate its effectiveness. Furthermore, the autonomous positioning of the UAV reduces human intervention, minimises inspection time, and increases efficiency and cost-effectiveness.*

Keywords

Autonomous positioning; UAV (Unmanned Aerial Vehicle); Power transmission lines; Insulator detection; Machine learning.

1. Introduction

With the rise in population and the country's development, the coverage of overhead transmission lines has continued to expand. Electricity has become a fundamental necessity for modern-day living, and the electricity demand is ever-increasing. This study focuses on the autonomous positioning of Unmanned Aerial Vehicles (UAVs) for power transmission line detection, to replace the traditional power transmission line inspection method, which poses significant danger. Using UAVs can reduce inspection costs, as fewer personnel are required for the task, and UAVs have a much lower cost than other vehicles like helicopters.

The efficiency and safety of autonomous UAVs in power transmission line inspection are affected by three key problem statements. Firstly, UAVs must stop automatically after detecting transmission line faults or

insulators to avoid taking unnecessary and memory-consuming photos. Fault detection accuracy is critical to prevent taking unusable photos or missing actual defects. Secondly, the UAV must be positioned correctly to capture clear photos by considering the trajectory consistency to optimise time, battery usage, and avoid collisions. Lastly, maintaining a safe distance from the power transmission line is crucial to prevent electromagnetic interference, UAV failure, collisions, and damage to both the UAV and the transmission line. Addressing these problems will improve the efficiency and safety of autonomous UAVs in power transmission line inspection.

This paper proposes a model for autonomously positioning UAVs to address the aforementioned shortcomings. Our contributions are: (i) A mathematical model is proposed to determine the optimal safety distance between the UAV and the target, (ii) In the model, machine learning techniques are implemented for autonomous detection of insulators on the transmission lines and identifying the best positions for capturing pictures, and (iii) The proposed model is validated by simulating the UAV's movement to the predicted optimal positions. This paper focuses on enhancing the UAV's ability to detect insulators, capture pictures from optimal positions, and maintain a suitable distance from the transmission lines, improving its power transmission line detection performance.

The outline of this paper is organised as follows. Section 2. provides background information on autonomous UAV positioning approaches. Section 3. details the proposed model, including machine learning for insulator detection, optimal distance between UAV and target, and UAV model simulation. The findings and analysis are presented in Section 4. . Finally, Section 5. draws a conclusion based on the results obtained.

2. Related Work

This section employs three distinct perspectives to examine the methods employed for the autonomous positioning of UAVs. Firstly, the circular trajectory of UAV movement is studied. Secondly, the mechanism for capturing images of transmission lines is explored. Lastly, the mechanism for estimating the position of UAVs is studied.

To achieve circular trajectory movement for UAVs, the autopilot control approach uses waypoint navigation, which considers the aircraft's longitude and latitude as Cartesian coordinates [2]. Another study uses force formulas, design parameters, and Newton-Euler motion to create a UAV movement model [3]. The model includes parameters such as the three-dimensional distance from a fixed origin to the drone's centre of mass and Euler angles. The Logarithmic Barrier Lyapunov Functions (BLF) is utilised in [4] to achieve circular motion for various types of vehicles, including aerial, ground, and underground vehicles. Other than that, an approximation of the Bernstein-Bezier polynomial and Pythagorean Hodograph is demonstrated in [5] for the curve trajectory of the UAV. However, a significant limitation is found in these studies. The UAVs may have difficulty taking photos at the lower portion of the power transmission line, as UAVs need to flip around their body to expose the camera to the area that needs to be photographed, which can be inefficient. Besides, Kwon, Ahn and Song [6] presented a circular route trajectory blending method that considers the end position effector's and orientation trajectories' temporal synchronisation. This algorithm includes the waypoint's position, orientation, velocity, and angular velocity parameters, which are time-synchronised. Another study in [7] presented circular path planning using posture control for six degrees of freedom. Two schemes were used here: Cartesian space and Joint space. The motion model was generated using piece-wise quintic polynomials with ongoing jerk curves.

In order to successfully capture images of faulty transmission lines using UAVs, an accurate detection mechanism is necessary. In [8], a solution for detecting transmission line faults using embedded chip-based quality optimisation is proposed. The reflection and coefficients of the transmission line were derived, and the attenuation rules of voltage and current waves were explained here. However, further study is necessary to determine the effectiveness of this method in different environments. Besides, [9, 10] studied the YOLOv4 algorithm in fault detection on power transmission lines. Due to the extensive database, deep learning-based detection algorithms provide precise and fast results. However, this comes with the downside of requiring large amounts of memory and bandwidth. In addition, sensors such as magneto-resistive and non-contact voltage for voltage monitoring and near-field voltage detection in power transmission lines are discussed in [11] and [12], respectively.

Researchers have studied different mechanisms and models to estimate the position of UAVs. Two examples are [9] and [13], which utilise GPS technology to guide the UAV toward the nearest power transmission line. They adopt different methods to determine the distance between the UAV and the power line. Besides, the Beidou navigation system, a form of GPS developed by China, is used in conjunction with other positioning methods to estimate the position of UAVs [14]. Furthermore, a vision-based system is implemented in [15–17] to detect the location of the UAV from the power line. In order of the image processing, Schofield,

	Images	X-coordinate	Y-coordinate of th	Center Point of In	Insulator's Label Coordinates (x1,y1,x2,y2)
2	Downloads/InsulatorDataSet-t	540.5	293.5	(540.5,293.5)	(96,228,985,359)
3	Downloads/InsulatorDataSet-t	492	289	(492,289)	(53,412,931,166)
4	Downloads/InsulatorDataSet-t	428	259.5	(428,259.5)	(93,256,763,263)
5	Downloads/InsulatorDataSet-t	386.5	301	(386.5,301)	(175,507,598,95)
6	Downloads/InsulatorDataSet-t	394	247	(394,247)	(153,377,635,117)
7	Downloads/InsulatorDataSet-t	447.5	379	(447.5,379)	(72,138,823,620)
8	Downloads/InsulatorDataSet-t	517.5	312	(517.5,312)	(138,261,897,363)
9	Downloads/InsulatorDataSet-t	495	302	(495,302)	(158,184,832,420)
10	Downloads/InsulatorDataSet-t	413	373.5	(413,373.5)	(365,613,461,134)
11	Downloads/InsulatorDataSet-t	498.5	380.5	(498.5,380.5)	(130,317,867,444)
12	Downloads/InsulatorDataSet-t	521	254	(521,254)	(55,162,987,346)
13	Downloads/InsulatorDataSet-t	520	288	(520,288)	(89,467,951,109)
14	Downloads/InsulatorDataSet-t	463	286	(463,286)	(85,317,841,255)
15	Downloads/InsulatorDataSet-t	416.5	361	(416.5,361)	(38,433,795,289)
16	Downloads/InsulatorDataSet-t	514.5	316	(514.5,316)	(32,428,997,204)
17	Downloads/InsulatorDataSet-t	492.5	330	(492.5,330)	(153,517,832,143)
18	Downloads/InsulatorDataSet-t	568	255	(568,255)	(85,258,1051,252)
19	Downloads/InsulatorDataSet-t	541	288.5	(541,288.5)	(107,457,975,120)
20	Downloads/InsulatorDataSet-t	530	282	(530,282)	(144,426,916,138)
21	Downloads/InsulatorDataSet-t	540	255.5	(540,255.5)	(102,341,978,170)
22	Downloads/InsulatorDataSet-t	504	228	(504,228)	(46,264,962,192)
23	Downloads/InsulatorDataSet-t	490.5	331.5	(490.5,331.5)	(105,525,876,138)
24	Downloads/InsulatorDataSet-t	487.5	307	(487.5,307)	(63,337,912,277)
25	Downloads/InsulatorDataSet-t	480	219.5	(480,219.5)	(77,300,883,139)
26	Downloads/InsulatorDataSet-t	487	261	(487,261)	(7,263,967,259)

Fig. 1: Part of Training Data Set

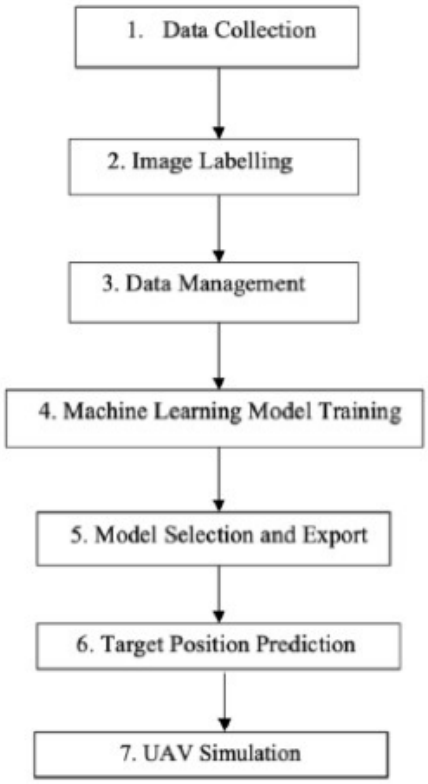

Fig. 2: Part of Training Data Set

Iversen, and Ebeid [15] use the LiDAR system, while Wang [16] uses the localisation and recognition of landmarks, as well as feature tracking among consecutive frames. According to Liu, Shao, Cai, and Li [17], the data obtained by LiDAR can be used to construct a path based on the secant slope properties of the power transmission line. In addition, the magnetic field is considered to determine the UAV's position from the power transmission line [18,19]. A positioning and navigation model for the UAV can be established based on the power transmission line's electric field strength distribution [20].

To summarise, there are several areas where research is needed to improve the use of autonomous positioning UAVs for power line detection. These include finding ways to capture images more efficiently during circular flight paths, improving fault detection mechanisms, reducing memory and bandwidth usage in detection algorithms, integrating various positioning technologies, developing real-time navigation algorithms, and creating comprehensive UAV positioning models. It is also important to develop strategies for adapting to different environmental conditions to ensure optimal UAV performance. Addressing these issues is essential for efficient and adaptable UAV operations in power line detection. Therefore, this paper focuses on determining the optimal positions for capturing the defective power transmission line insulators.

3. Methodology

3.1. Overall Procedure

This study involves several key steps: data collection, image labelling, data management, machine learning model training, model selection and export, insulator position prediction, and UAV simulation. Images with feature insulators from various online source was systematically collected. These images encompassed different angles, lighting conditions, and variations in insulator appearance to create a comprehensive training dataset. The images were then labelled using the 'Image Labeler' app within the MATLAB environment, allowing precise marking of the insulator's location and boundaries. The labelled information, including position coordinates and insulator attributes, was exported to the MATLAB workspace for further analysis and model training. The training set comprised 600 images. Within this dataset, each entry contained the images themselves along with the corresponding coordinates of their centre points, essential for determining optimal coordinates as shown in Figure 1.

The collected data was then managed and organised in a table format, facilitating subsequent data analysis and model training. The table contained various information such as image file paths, exported insulator label information, individual coordinates, and target centre point coordinates. The table served as the foundation for training the machine learning model.

The machine learning model training was conducted using MATLAB's 'Classification Learner' toolbox, the process was done offline. After evaluation, the selected machine learning models were used for prediction and further analysis. Two distinct models were trained: one to predict the centre point of the target insulator within an image and another to detect the size of the target. Three machine learning models were exported to pre-

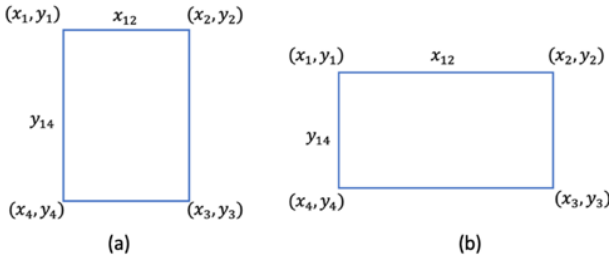

Fig. 3: Criteria for (a) $y_{14} > x_{12}$ and (b) $x_{12} > y_{14}$

dict the centre point. The results were compared to determine the most suitable model. The trained machine learning models were then used to predict the position of the target insulator in input images. Then, Simulink was used to verify the autonomous UAV model, as explained in Section 3.3. . Figure 2 shows the flowchart of overall procedure.

3.2. Mathematical Model for Optimal Distance Between UAV and Target

This step mainly calculates the optimal distance between the insulator and the camera for the best shooting position. Here, the size of the insulator appearing in the vision of the UAV should be maximised to obtain a good image for insulator defect detection later.

In order to determine the insulator size on the power transmission line, y_{14} and x_{12} are defined. y_{14} is the vertical length from y_1 to y_4, or y_2 to y_3, and x_{12} is the horizontal length from x_1 to x_2, or x_4 to x_3 as shown in Figure 2. The length of y_{14} and x_{12} is calculated by Equation (1) and Equation (2).

$$y_{14} = |y_1 - y_4|, \tag{1}$$

$$x_{12} = |x_1 - x_2|. \tag{2}$$

Based on the dataset's images, the optimal vertical length, y_{14} or y_{23}, and horizontal length, x_{12} or x_{43}, equals 800. The optimal length of 800 units is determined by finding the ideal size of the target as it appears in the image. This distance is optimal when the target occupies % of the captured image. Two criteria are set here: when y_{14} is longer than x_{12}, and x_{12} is longer than y_{14}, as shown in Figure 3 (a) and (b) respectively.

If $(y_{14} > x_{12})$ happens, the length of y_{14} will be considered. When y_{14} exceeds 800, the UAV is too near the insulator and must move away from the insulator until $y_{14} = 800$. Conversely, if the y_{14} is shorter than 800, the UAV must move closer to the insulator until $y_{14} = 800$ to get a clearer image. However, if $(x_{12} > y_{14})$ happens, the length of x_{12} will be considered. When x_{12} exceeds 800, the UAV is too close to the insulator and must move away from the insulator until $x_{12} = 800$. Conversely, if the x_{12} is shorter than 800, the UAV must move closer to the insulator until $x_{12} = 800$.

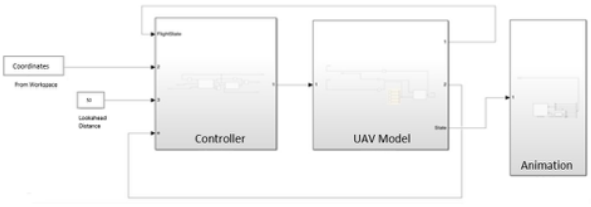

Fig. 4: UAV Simulation

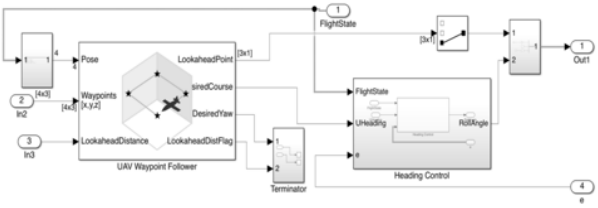

Fig. 5: Controller

3.3. UAV Simulation in Simulink

The UAV simulation model is developed using MATLAB Simulink, which has three main components: Controller, UAV Model and Animation. It involves connecting several blocks to establish the necessary functionality and visualisation, as shown in Figure 4.

The predicted coordinates from the machine learning algorithm were obtained from the workspace using the 'From Workspace' block. This block and a constant block are both connected to the Controller. The constant block is used to determine the lookahead distance, which determines how far ahead the UAV looks to anticipate and plan its trajectory.

In the Controller, the 'UAV Waypoint Follower' block received the coordinates and lookahead distance as input and generated the required information for heading control. The output ports 'Desired Yaw' and 'Look ahead Distance Flag' were connected to the terminator. The 'Heading Control' block processed the outputs from the 'UAV Waypoint Follower' block and produced the roll angle as its output, which served as the output of the Controller as shown in Figure 5.

The subsequent component, named UAV Model as shown in Figure 6, consists of the UAV guidance model, which provides environmental information. Their values are manipulated to observe the behaviour and trajectory of the UAV under different conditions. The environment information is also feedback to the Controller. The state of the UAV was the output of the UAV model.

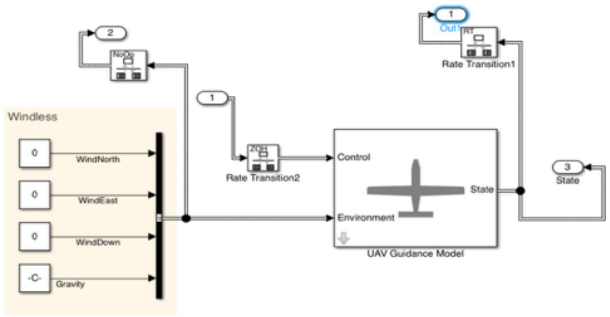

Fig. 6: UAV Model

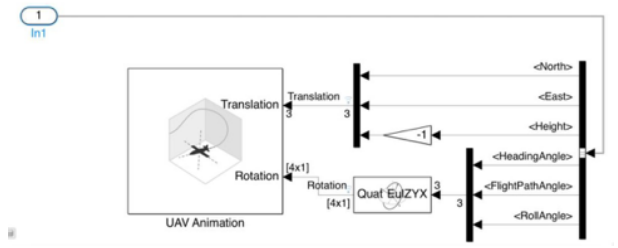

Fig. 7: Animation

The component of Animation incorporates the UAV Animation block, which facilitated the observation of the UAV's trajectory. The state information obtained from the UAV model is decoded and classified into 'Translation' and 'Rotation'. The 'Quaternion to Euler' block converts the angles into Euler format, enabling the 'UAV Animation' block to interpret the information and display the UAV's trajectory. For the algorithm of animation block, illustrating a UAV's trajectory through translations and rotations, this block visually depicts the UAV's flight path based on input translations and rotations relative to the inertial frame. Ensuring consistency, the plot's z-axis consistently points upwards irrespective of the inertial frame's z-axis orientation. Translation is encapsulated in a 3-element vector denoting the UAV's xyz-position relative to the inertial frame, while rotation is encapsulated in a 4-element quaternion vector signifying the UAV's rotation relative to the inertial frame. The detail of animation block is showed in Figure 7.

4. Result and Discussion

4.1. Insulator Detection

The insulator's predicted coordinates are presented here, which were obtained using three different machine learning models: Naive Bayes, support vector machine (SVM), and Decision Tree. Figure 8 displays the ground truth coordinates of the target in Image A while Figure 9 indicates the predicted coordinates in Image A by Naive Bayes, SVM and Tree Decision.

Fig. 8: Animation

The process of predicting the coordinates, as shown in Figure 8, is replicated to determine the target's coordinates in the remaining images. The resulting ground truth and predicted coordinates are then documented in Table 1.

Tab. 1: Distribution of the types by rank.

Image	Ground Truth Coordinates	Predicted Coordinates(x,y)		
		Naive Bayes	SVM	Tree Decision
Image A	(511.5, 477)	(511.5, 460)	(511.5, 360)	(517.5, 299.5)
Image B	(480.5, 390)	(470.5, 360)	(500.5, 219.5)	(487.5, 291.5)
Image C	(505, 471)	(500, 460)	(463.5, 298)	(305.5, 361)
Image D	(425, 475)	(425, 475)	(473, 290)	(306.5, 361)
Image E	(517.5, 305.5)	(517.5, 299.5)	(565, 242)	(487.5, 291.5)

To evaluate the accuracy and efficiency of the prediction, the Euclidean distance is calculated between the actual values and the predicted coordinates as shown in Table 2. The Euclidean distance serves as a quantitative measure to assess the level of agreement between the predicted and actual coordinates, providing valuable insights into the performance of the different machine learning models in accurately predicting the target locations. The Euclidean Distance can be calculated using the Equation (3):

$$Distance = \sqrt{(x_2 - x_1)^2 + (y_2 - y_1)^2}. \quad (3)$$

These observations highlight the varying performance of the three machine learning models in predicting the target coordinates. The Naive Bayes model stood out for its overall accuracy, while the SVM model exhibited greater consistency, particularly in the x-coordinate predictions. The SVM model may have exhibited greater consistency, particularly in x-coordinate predictions, due to its robustness to

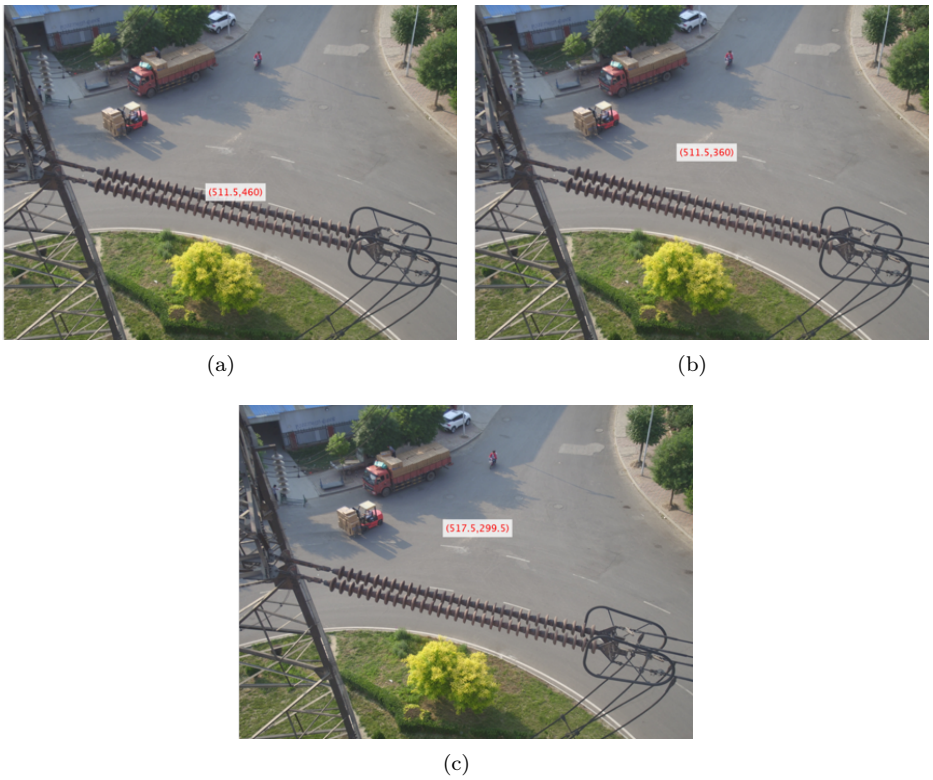

(a) (b)

(c)

Fig. 9: Predicted Coordinates in Image A by (a) Naive Bayes (b) SVM (c)

Tab. 2: Distribution of the types by rank.

Image	Euclidean Distance between Actual Coordinates and Predicted Coordinates		
	Naive Bayes	SVM	Tree Decision
Image A	17	117	177.6
Image B	31.6	171.7	98.7
Image C	12.1	177.9	227.8
Image D	0	191.1	164.4
Image E	6	79.3	33.1

Tab. 3: Distribution of the types by rank.

Image	Q / unit	Z Coordinate
Image A	597	-20.30
Image B	793	-0.70
Image C	537	-26.30
Image D	836	3.60
Image E	884	8.40

outliers, effective handling of non-linear relationships through kernel functions, optimization of margin separation, and ability to handle high-dimensional data. By maximizing the margin between different classes and finding the optimal hyperplane in the feature space, SVMs can provide more robust and generalizable predictions, especially in tasks involving coordinate predictions where data may be high-dimensional and non-linear relationships may exist. The limitations and strengths of each model should be considered when selecting the most suitable model for similar tasks or further improving the prediction accuracy in future applications.

Table 3 presents the recorded values of the z coordinate for the predicted coordinates, which play a crucial role in determining the zoom level for the system. The table includes the z coordinate itself and the corresponding Q value, representing the target size observed in the images. The relationship between the z coordinate and Q value is calculated using a specific method, as demonstrated in the part of Code Implementation Details. This table provides valuable insights into the zooming mechanism and its correlation with the predicted coordinates, contributing to the system's overall functionality.

The Z-coordinate is found using Equation (4). In this context, 800 units represent the desired size of the target appearing in the images. Considering an assumption where each unit increase in UAV altitude corresponds to a 10-unit increase in the size of the insulator in the image, the difference between Q and 800 is divided by 10 to account for this relationship. The target's size within the image should ideally represent 4/5 of the entire image size. While the target's size may vary depending on the UAV or camera used for image capture, in the context of the dataset, an optimal size of 800 units ensures that the target appears appropriately in the image, neither too distant nor too

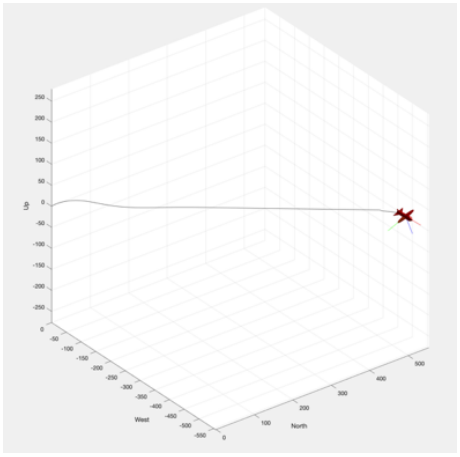

Fig. 10: UAV Simulation Based on coordinates Predicted in Image A

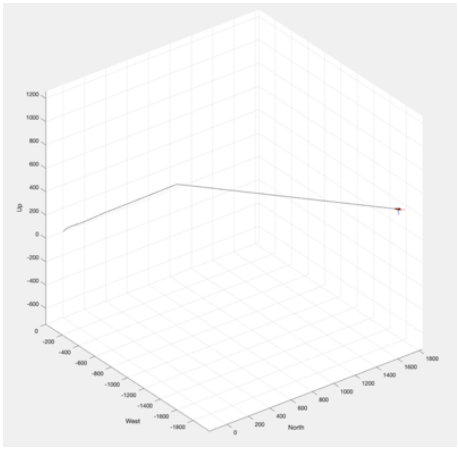

Fig. 11: UAV trajectory in a Windless Environment

close to the UAV.

$$z = \frac{Q - 800}{10}, \tag{4}$$

To maximize the size of the insulator in the UAV's vision while accounting for the UAV's speed, careful coordination between the UAV's movement and the distance to the target is necessary. If the UAV's speed causes the distance to exceed 800, adjustments must be made to maintain the optimal distance. In this scenario, the UAV would need to slow down or change direction to reduce the deviation and ensure that the insulator remains within the desired range of visibility. By dynamically adjusting its trajectory, the UAV can effectively manage its speed to maintain optimal viewing conditions for insulator detection.

Among the images analysed, Images A, B, and C exhibit z-coordinates with negative values based on Table 3, indicating that the UAV is progressively approaching these targets. Conversely, for Images D and E, the UAV moves away from the target to maintain a consistent target size within the images. By carefully evaluating the z coordinates, the UAV can effectively regulate its distance from the targets, ensuring accurate and consistent observations throughout the mission.

4.2. UAV Simulation in Simulink

The results of the UAV Simulation in Simulink provide a visual representation of the UAV's flight path as it navigates towards the target coordinates by following predefined waypoints. The initial x, y and z coordinates are set to zero to establish the origin. Building upon the previous section of the results, the coordinates of the target in Image A, which the Naïve Bayes model predicted, are used to simulate the UAV and the result is shown in Figure 10. The first set of results showcases the UAV's trajectory in the default environment setting, characterised by calm wind conditions.

To further explore the UAV's behaviour under different conditions, variations in the wind values are introduced, and the trajectory waypoints serve as a constant variable in this section. By manipulating the wind parameters, the way that the UAV's flight path is influenced and its ability to adapt to changing environmental factors can be observed. These simulations provide valuable insights into the UAV's performance and enable a comprehensive analysis of its behaviour in various scenarios. Figure 10 to Figure 17 indicate the trajectory of UAV under different wind conditions.

Under the wind direction solely northward, the UAV exhibited a slightly snakelike trajectory when travelling perpendicular to the north axis. However, it travelled smoothly when moving north, resulting in a shorter time to reach the final point than the windless scenario. This can be attributed to the northward wind "pushing" the UAV, enabling faster flight. When the wind direction was solely in the eastward direction, the UAV changed its trajectory and reached the final point in a shorter time. Conversely, in the presence of a downward wind, the trajectory resembled that of the windless environment, but the time required to reach the final point was longer, as indicated in Table 4.

Tab. 4: Distribution of the types by rank.

Wind Direction	Time (sec)
Windless	200
Northward	190
Eastward	180
Downward	250
Northward and Eastward	200
Northward and Downward	300
Eastward and Downward	500

Further analysis focused on the effects of wind in two directions. When both northward and eastward winds were applied, the UAV's trajectory became highly er-

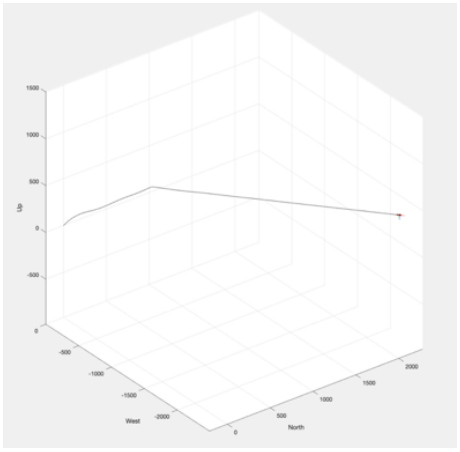

Fig. 12: UAV Trajectory under Northward Wind Condition

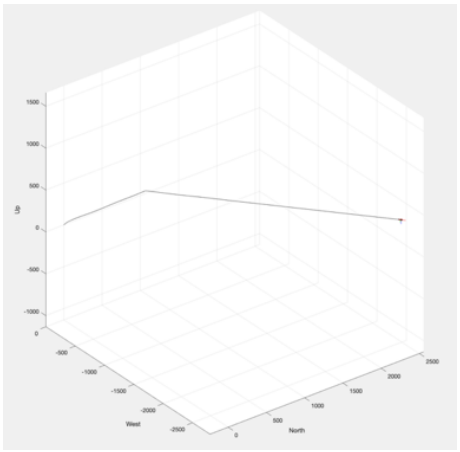

Fig. 13: UAV Trajectory under Eastward Wind Condition

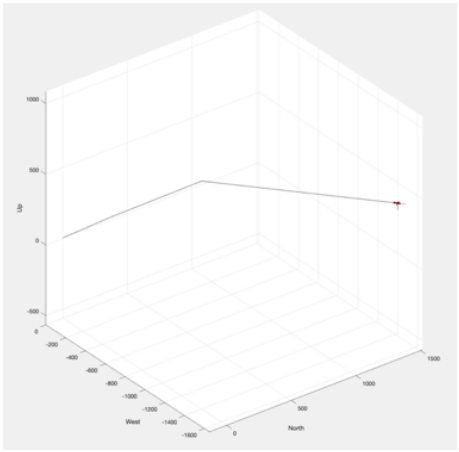

Fig. 14: UAV Trajectory under Downward Wind Condition

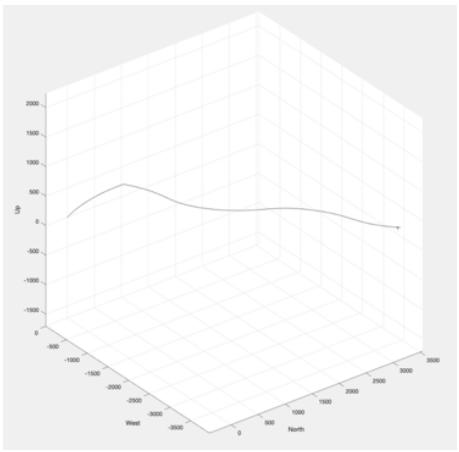

Fig. 15: UAV Trajectory under Northward and Eastward Wind

ratic, deviating from the target point. Similarly, when both northward and downward winds were present, the trajectory exhibited initial instability but later became smoother. However, the time required to reach the final point was significantly longer in this scenario. Finally, with eastward and downward winds, the UAV's trajectory was most affected when travelling in the north direction (perpendicular to the eastward wind), and it took the longest time to reach the target.

In short, the UAV demonstrated faster travel when moving parallel and in the same direction as the wind, while perpendicular travel to the wind resulted in trajectory deviations. Among the analysed wind directions, the downward wind had the most significant impact on the time required for the UAV to reach its final position.

5. Conclusion

The main objective of this study was to enhance the inspection of power transmission lines by developing an autonomous Unmanned Aerial Vehicle (UAV) system. During the research, certain gaps in the existing literature were identified, such as the optimal distance between the UAV and the transmission line and the challenges of capturing clear photos. The research team addressed these gaps by introducing a methodology that involves machine learning for insulator detection and simulation modelling for UAV positioning. In this simulation, the UAV's behaviour is significantly influenced by environmental elements such as changing wind speed and direction. Although factors like temperature and sunlight intensity were not investigated in this study, they could be potential avenues for future research in this field. Additionally, further considerations, such as integrating features for natural disaster conditions, should be explored in upcoming studies. The results of this study showed that the approach was effective in enhancing the accuracy of insulator detection and assessing the impact of wind on UAV trajectory. Overall, this study improves UAV technology in power transmission line inspection, which can significantly enhance the efficiency and reliability of maintaining power infrastructure.

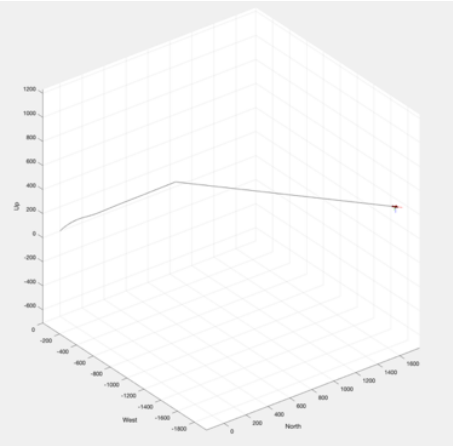

Fig. 16: UAV Trajectory under Northward and Downward Wind

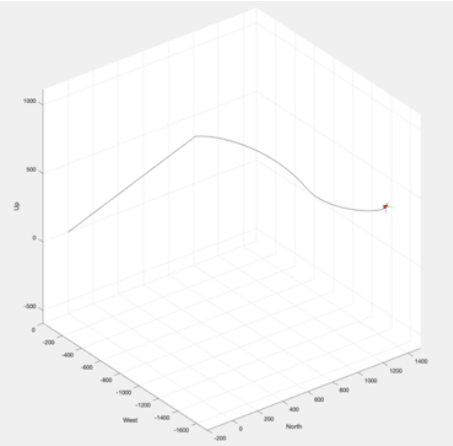

Fig. 17: UAV Trajectory under Eastward and Downward Wind

Acknowledgment

The authors would like to acknowledge the Faculty of Engineering, Universiti Malaysia Sarawak for the support in preparing this article.

Author Contributions

Sze Sin VOON developed the methodology and simulation. Annie JOSEPH was responsible for validating the research findings. Sze Song NGU and Kuryati KIPLI contributed to reviewing and editing the manuscript. Lee Chin KHO supervised the research.

References

[1] LI, X., Z. LI, H., WANG and LI, W. Unmanned Aerial Vehicle for Transmission Line Inspection: Status, Standardization, and Perspectives. In: *Front Energy Res*. Kunming: Frontier, 2021, vol. 9. DOI: 10.3389/fenrg.2021.713634.

[2] DECICCO, N., K. NAPOLITANO, R. TRAFFORD, P. GEORGIEVA, N. BOUAYNAYA and R. POLIKAR. Trajectory design of an Aircraft for Circular Motion. In: *IEEE International Conference on Control and Automation, ICCA*. Singapore: IEEE, 2020, pp. 373–377. ISBN 978-1-7281-9094-5. DOI: 10.1109/ICCA51439.2020.9264537.

[3] YASAR, S. N., and E. KARAKOSE. Trajectory Control of Quadcopter in Matlab Simulation Environment. In: *2022 International Conference on Decision Aid Sciences and Applications, DASA*. Chiangrai: IEEE, 2022, pp. 1127–1131. ISBN 978-1-6654-9502-8. DOI: 10.1109/DASA54658.2022.9765119.

[4] SHARMA, S., and JAIN, A. Collective Circular Motion with Trajectory and Turn-Rate Constraints. In: *7th Indian Control Conference, ICC 2021 – Proceedings*. Mumbai: IEEE, 2021,pp. 225–230. ISBN 978-1-6654-0979-7. DOI: 10.1109/ICC54714.2021.9703143.

[5] VINOKURSKY, D. L., O. S. MEZENTCEVA and P. V. SAMOYLOV. Trajectory Planning of UAV Group: Pythagorean Hodograph and Bernstein-Bezier Composite Curves in the Plane. In: *Proceedings - International Russian Automation Conference, RusAutoCon*. Sochi: IEEE, 2020, pp. 704–707. ISBN 978-1-7281-6131-0. DOI: 10.1109/RUSAUTOCON49822.2020.9208121.

[6] KWON, H., K. H. AHN and J. B. SONG. Circular Path Based Trajectory Blending Algorithm Considering Time Synchronization of Position and Orientation Trajectories. In: *15th International Conference on Ubiquitous Robots, UR*. Honolulu: IEEE, 2018, pp. 847–851. ISBN 978-1-5386-6335-6. DOI: 10.1109/URAI.2018.8441777.

[7] LI, J., M. GAO, Z. HE, and Y. YANG. Circular trajectory planning with pose control for Six-DOF manipulator. In: *Proceedings of 2018 IEEE 4th Information Technology and Mechatronics Engineering Conference, ITOEC*. Chongqing: IEEE, 2018, pp. 1950–1955. ISBN 978-1-5386-5374-6. DOI: 10.1109/ITOEC.2018.8740503.

[8] ZHAO, H. et al. Quality Optimization of Transmission Line Fault Detection Algorithm based on Embedded Chip. In: *Proceedings - International Conference on Control Science and Electric Power Systems, CSEPS*. Shanghai: IEEE, 2021, pp. 79–82. ISBN 978-1-6654-2618-3. DOI: 10.1109/CSEPS53726.2021.00023.

[9] LOPEZ, R. L., M. J. B. SANCHEZ, M. P. JIMENEZ, B. C. ARRUE, and A. OLLERO. Autonomous UAV System for Cleaning Insulators in Power Line Inspection and Maintenance. *Sensors*. 2021, vol. 21, no. 24. DOI: 10.3390/s21248488.

[10] DENG, F. et al. Research on edge intelligent recognition method oriented to transmission line insulator fault detection. *International Journal of Electrical Power & Energy Systems*. 2022, vol. 139, p. 108054. DOI: 10.1016/J.IJEPES.2022.108054.

[11] ZHU, K., W. K. LEE, and P. W. T. PONG. Non-Contact Voltage Monitoring of HVDC Transmission Lines Based on Electromagnetic Fields. *IEEE Sensors Journal*. 2019, vol. 19, no. 8, pp. 3121–3129. ISBN 1558-1748. DOI: 10.1109/JSEN.2019.2892498.

[12] LI, S., W. PENG, Q. ZHOU, and X. HOU. Researc on Non-contact Voltage Measurement Technology Based on Near Field Detection. In: *iSPEC 2019 - 2019 IEEE Sustainable Power and Energy Conference: Grid Modernization for Energy Revolution, Proceedings*. Beijing: IEEE, Nov. 2019, pp. 2704–2707. ISBN 978-1-7281-4931-8. DOI: 10.1109/ISPEC48194.2019.8974904.

[13] TAKAYA, K., H. OHTA, V. KROUMOV, K. SHIBAYAMA, and M. NAKAMURA. Development of UAV system for autonomous power line inspection. In: *23rd International Conference on System Theory, Control and Computing, ICSTCC*. Sinaia: IEEE, 2019, Proceedings. ISBN 2372-1618. DOI: 10.1109/ICSTCC.2019.8885596.

[14] HU, H, H. ZHOU, J. LI, K. LI, and B. PAN. Automatic and Intelligent Line Inspection using UAV based on Beidou Navigation Systém. In: *Proceedings - 2019 6th International Conference on Information Science and Control Engineering, ICISCE*. Shanghai: IEEE, 2019, pp. 1004–1008. ISBN 978-1-7281-5713-9. DOI: 10.1109/ICISCE48695.2019.00202.

[15] SCHOFIELD, O. B., N. IVERSEN and E. EBEID. Autonomous power line detection and tracking system using UAVs. *Microprocess Microsyst*. 2022, vol. 94, p. 104609. DOI: 10.1016/J.MICPRO.2022.104609.

[16] WANG, J. Autonomous Localization and Navigation for Transmission Line Inspection of UAV. In: *IEEE International Conference on Advances in Electrical Engineering and Computer Applications, AEECA*. Dalian: IEEE, 2021, pp. 98–104. ISBN 978-1-6654-0257-6. DOI: 10.1109/AEECA52519.2021.9574359.

[17] LIU, C., Y. SHAO, Z. CAI, and Y. LI. Unmanned Aerial Vehicle Positioning Algorithm Based on the Secant Slope Characteristics of Transmission Lines. *IEEE Access*. 2002, vol. 8, pp. 43229–43242. ISSN 2169-3536. DOI: 10.1109/ACCESS.2020.2977923.

[18] WU, Y., Y. LUO, G. ZHAO, J. HU, F. GAO, and S. WANG. A Novel Line Position Recognition Method in Transmission Line Patrolling with UAV using Machine Learning Algorithms. In: *IEEE International Symposium on Electromagnetic Compatibility and IEEE Asia-Pacific Symposium on Electromagnetic Compatibility, EMC/APEMC*. Singapore: IEEE, 2018, pp. 491–495. ISBN 978-1-5090-3955-5. DOI: 10.1109/ISEMC.2018.8393827.

[19] WU, Y. et al. Overhead Transmission Line Parameter Reconstruction for UAV Inspection Based on Tunneling Magnetoresistive Sensors and Inverse Models. *IEEE Transactions on Power Delivery*. 2019, vol. 34, no. 3, pp. 819–827. ISSN 1937-4208. DOI: 10.1109/TPWRD.2019.2891119.

[20] LI, Y., W. Z HANG, P. LI, Y. NING, and C. SUO. A Method for Autonomous Navigation and Positioning of UAV based on Electric Field Array Detection. *Remote Sensors*. 2021, vol. 21, no. 4. DOI: 10.3390/s21041146.

[21] N. Dhananjay and D. Ghose. Accurate Time-to-Go Estimation for Proportional Navigation Guidance. *Journal of Guidance, Control and Dynamics*. 2014, vol. 37, no. 4, pp. 1378–1383. DOI: 10.2514/1.G000082.